CHAPTER FIVE
CARBON AND OXYGEN ISOTOPES

5.1 Introduction

Oxygen and carbon isotopes are well established as proxies of palaeoclimatic change during the Quaternary and robust records for these changes exist from deep sea cores of ocean sediments, ice cores and speleothems. Speleothems are particularly good reservoirs of climatic data, which is enhanced by their inherent ability to be easily and accurately dated via Uranium-series (Chapter 4). This chapter examines the results of the direct stable light isotope analysis of the Gladysvale flowstones and breccias within the FBU, as well as a number of modern samples.

5.2 Standards

In order to calibrate samples, standards of known isotopic composition are analysed along with each run of samples. In this study internal laboratory samples Cavendish marble and Carrara Z and international standard NBS 18 were chosen (see Table 2.2 for carbon and oxygen isotope values of standards).

5.2.1 Data

The raw results for $\delta^{13}C$ and $\delta^{18}O$ for the standards are summarised in Table 5.1. The mean and standard deviation for each standard are calculated. The mean is used for the calibration of the samples and the standard deviation is a measure of the error on the samples. The error on the carbon values for all three standards are very low, with standard deviations of 0.055 to 0.137. The oxygen has slightly larger errors, with standard deviations of 0.208 to 0.275.

5.2.2 Calibration

Samples are calibrated using the measured $\delta^{13}C$ and $\delta^{18}O$ values for the standards and comparing these to the known isotope values of the standards (Table 5.2). All the isotope values are reported with respect to PeeDee Belemnite (PDB) and expressed as ‰ values.

Run no.	Sample	Mass (mg)	SA44 (V)	$\delta^{13}C$ raw	$\delta^{18}O$ raw
1	Cavendish marble	0.071	2.902	9.195	-6.865
	Cavendish marble	0.071	3.979	9.284	-7.355
2	Cavendish marble	0.083	4.881	9.247	-7.326
	Cavendish marble	0.084	5.872	9.389	-6.805
3	Cavendish marble	0.084	5.761	9.228	-7.223
	Cavendish marble	0.084	6.891	9.306	-6.910
4	Cavendish marble	0.085	5.909	9.284	-7.159
	Cavendish marble	0.080	6.084	9.304	-7.084
	Cavendish marble	0.072	6.296	9.280	-6.896
			mean	**9.280**	**-7.069**
			std dev	**0.055**	**0.208**
1	Carrara Z	0.073	3.703	11.013	0.170
2	Carrara Z	0.087	4.586	11.010	0.073
	Carrara Z	0.081	3.715	11.110	-0.343
4	Carrara Z	0.080	5.439	11.017	-0.121
	Carrara Z	0.084	6.988	11.125	0.374
			mean	**11.055**	**0.031**
			std dev	**0.057**	**0.275**
5	NBS 18	0.081	5.170	3.787	-23.353
	NBS 18	0.078	4.939	3.545	-23.747
	NBS 18	0.078	4.848	3.617	-23.337
	NBS 18	0.081	4.543	3.465	-23.741
			mean	**3.604**	**-23.545**
			std dev	**0.137**	**0.230**

Table 5.1. Raw $\delta^{13}C$ and $\delta^{18}O$ data for standards Cavendish marble, Carrara Z and NBS 18.

Standard	$\delta^{13}C$ raw	$\delta^{13}C$ PDB	Difference	Check	$\delta^{18}O$ raw	$\delta^{18}O$ PBD	Difference	Check
Cavendish marble	9.28	0.34	8.94	0.44	-7.069	-8.95	1.881	-8.26
Carrara Z	11.06	2.25	8.805	2.17	0.031	-1.27	1.301	-1.75
NBS 18	3.62	-5.05	8.666	-5.07	-23.422	-23.03	-0.392	-23.24

Table 5.2. Calibration of known standards Cavendish marble, Carrara Z and NBS.

The difference between the measured and expected results is calculated and is a measure of the drift within the mass spectrometer during the run. The difference in the carbon values is between 8.6 and 8.9 ‰, showing that, while there is an amount of internal fractionation during analysis, the amount of fractionation is almost equal for the different standards. The difference in the oxygen values is between -0.3 and 1.8, which covers a larger interval, suggesting that there is differential fractionation during analysis for the different standards. The known values and the means of the measured values for carbon and oxygen are graphed against each other, and the equation of the trend line is used to calibrate the samples, where the raw sample value is substituted for X (Figure 5.1). This equation is checked by substituting the raw values for the standards and comparing the calibrated value for the standards against the known value.

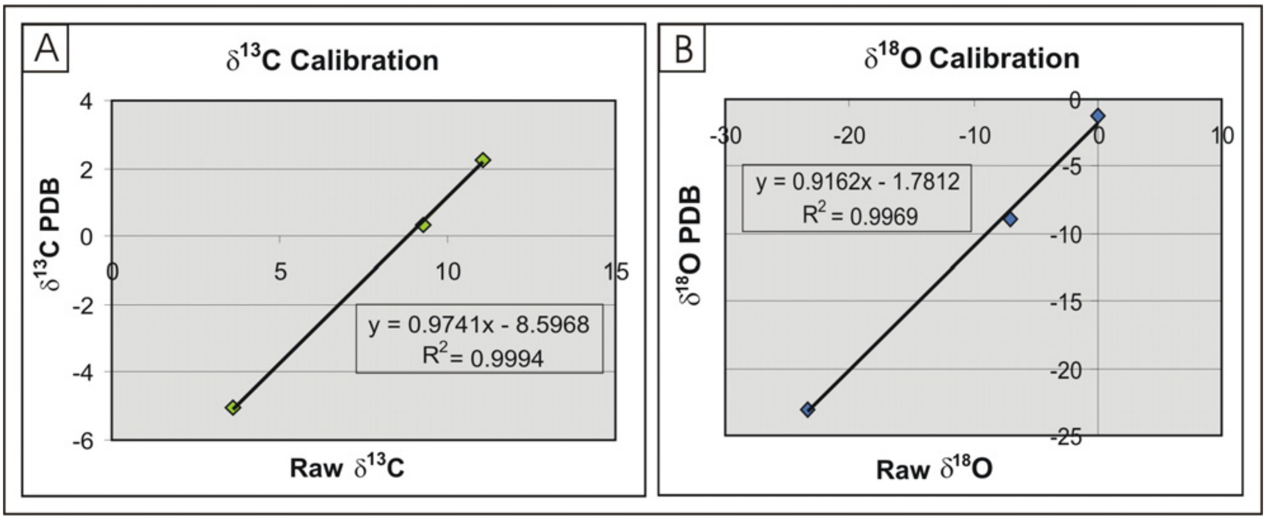

Figure 5.1. Calibration curves for δ^{13}C (A) and δ^{18}O (B).

5.3 Background stable light isotope data

Samples of cave roof dolomite, modern flowstone and recent stalactites from Gladysvale Cave were analysed in order to build up a background data set in which to better interpret the stable light isotope values of the flowstone and breccias. The data are presented in Table 5.3.

Sample	Comment	Mass (mg)	SA44 [V]	Raw δ^{13}C vs PDB	Corrected δ^{13}C vs PDB	Raw δ^{18}O vs PDB	Corrected δ^{18}O vs PDB
RP 22R	Cave roof dolomite	0.080	5.235	8.786	0.0	-2.897	-4.4
RP 20	Modern flowstone	0.085	6.076	0.430	-8.2	-0.621	-2.4
RP 20A	Modern flowstone	0.080	6.818	0.517	-8.1	-0.438	-2.2
RP 21	Modern flowstone	0.083	5.980	0.602	-8.0	-0.379	-2.1
RP 14	Mod 1 base	0.083	4.017	22.535	13.4	7.468	5.1
RP 14R	Mod 1 base	0.082	5.001	22.582	13.4	6.636	4.3
RP 15	Mod 1 tip	0.085	5.261	2.110	-6.5	0.503	-1.3
RP 16	Mod 2 base	0.081	4.818	7.528	-1.3	1.302	-0.6
RP 17	Mod 2 tip	0.082	4.692	1.355	-7.3	0.939	-0.9
RP 18	Mod 3 base	0.081	5.407	7.048	-1.7	1.976	0.0
RP 19	Mod 3 tip	0.082	5.592	2.415	-6.2	0.981	-0.9

Table 5.3. Stable light isotope data for modern stalactites, flowstone and cave roof dolomite.

5.3.1 Dolomite

The dolomite sample was analysed in order to determine the stable light isotope signature of the cave roof, to assess whether the ground waters feeding the calcium carbonate samples inside the cave are affected by their passage through the cave roof.

The carbon signal in dolomites is determined by that of the original carbonate, pre-dolomitisation. The $\delta^{13}C$ signal of Gladysvale dolomite is 0 ‰ (Table 5.3), which is to be expected for marine carbonates (Faure, 1986; Tucker & Wright, 1990; Hoefs, 1997). The oxygen signal in dolomites is, however, more complex and is acquired during the process of dolomitisation, which occurs in the presence of water, so much of the $\delta^{18}O$ signal of dolomite is from the pore fluid composition and the temperature of formation of the dolomite (Hoefs, 1997). As a result the oxygen signal of dolomites varies hugely and there is no typical value. The $\delta^{18}O$ signal for the Gladysvale dolomite is -4.4 ‰ (Table 5.3), which must reflect the conditions of formation of this particular dolomite within the Malmani Subgroup suite of dolomites.

5.3.2 Flowstone

A modern flowstone at Gladysvale is growing on the floor below the Hinge area of the cave (see Figure 2.1), and covers an area of about 1m^2 (Figure 5.2 A). There are a number of other small flowstone patches in the central, more protected areas of the upper chamber (Figure 5.2 B). The cave was observed actively dripping during the wet summer months of December through to February of 2002/2003, but during 2003/2004 drought conditions caused the cessation of drip waters in the upper chamber at Gladysvale.

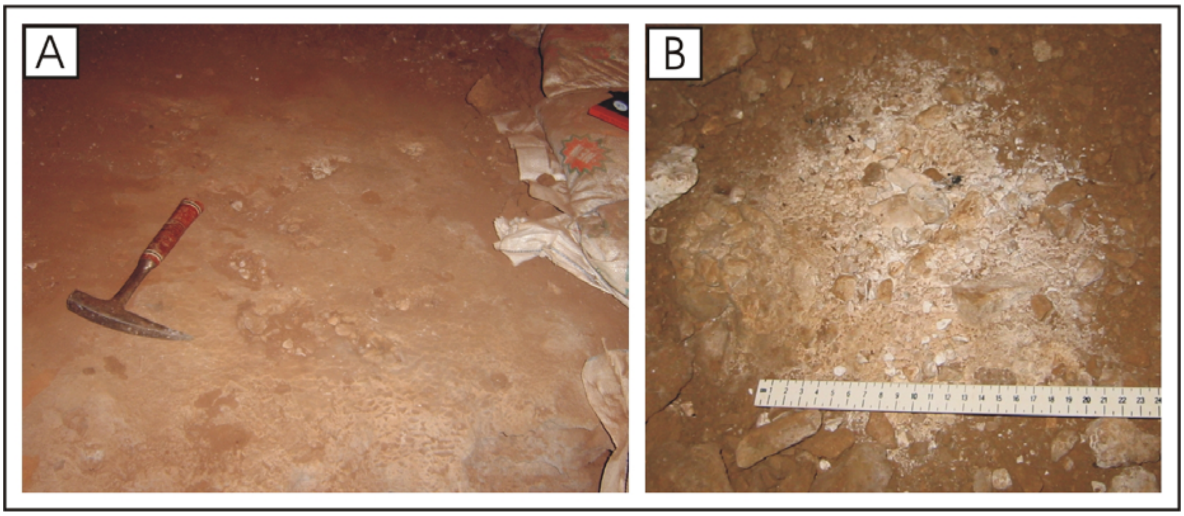

Figure 5.2. Modern flowstone currently growing during wet months at Gladysvale. A: modern flowstone sampled for stable light isotopes (30cm geopick for scale), B: smaller patch of modern flowstone (centimetre graded ruler for scale).

The carbon signal for the modern flowstone is -8.1 ‰ (Table 5.3). Using Talma and Vogel's (1992) estimation of the vegetation type from the $\delta^{13}C$ values, -8.1 ‰ equates to just over 30% C3 vegetation. The modern flowstone samples give a reasonably negative oxygen signal of ~-2.2 ‰ (Table 5.3). Gladysvale Cave is much more open today than it ever was in the past, as the lime miners have significantly increased the size of the cave entrances. This has produced more evaporative conditions within the cave, which are probably responsible for the negative oxygen signal of the modern flowstone, rather than any rainfall variation.

5.3.3 Stalactites

During the 1920's Gladysvale Cave was mined extensively for the speleothem formation within the cave, and the large stalactites formed along the two major fault lines in the roof were broken off, leaving stumps behind. The largest stalactite clusters occur on the section of cave roof between the Generator section and the Porcupine Pit (see Figure 2.1). This area of the cave still receives drip waters during the wet summer months, and small straws and stalactites have grown down from the stumps of the broken off stalactites (Figure 5.2). Mining ceased in 1928 (Berger & Tobias, 1994), giving these little stalactites a minimum age of 76 years. Three stalactites, on average 4cm long, were very carefully sampled for stable light isotope analysis. Samples were taken from the base and tip of each stalactite and analysed for carbon and oxygen isotopes.

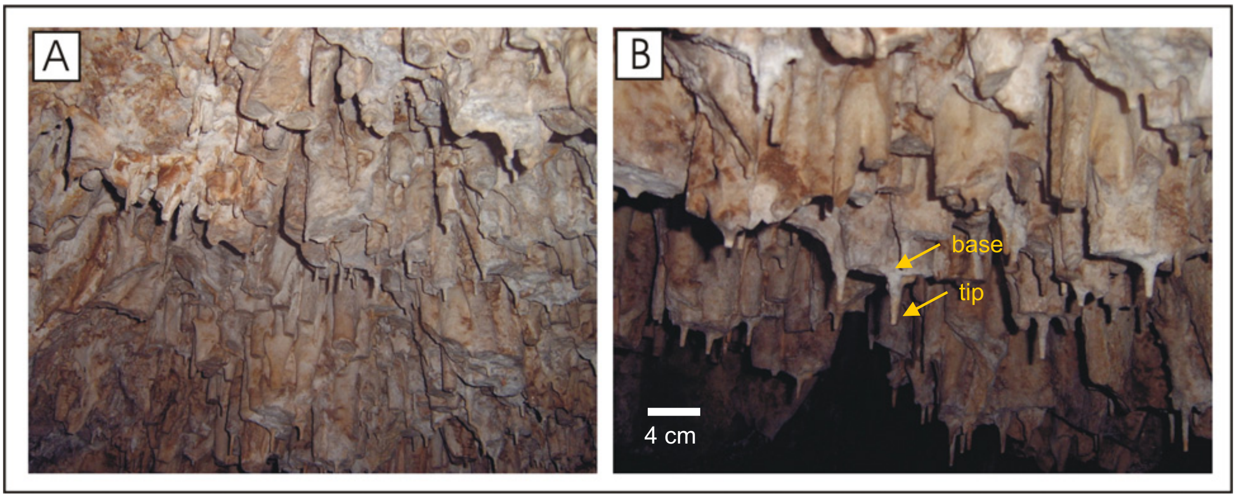

Figure 5.2. Modern stalactites growing on the stumps of older stalactites, which were broken off during mining of the cave in the 1920's.

The carbon and oxygen isotope values for the three stalactites analysed (Table 5.3) show huge variation and are very different from the other samples. To asses the possible affect of kinetic fractionation, the $\delta^{13}C$ and $\delta^{18}O$ values are graphed against each other (Figure 5.4).

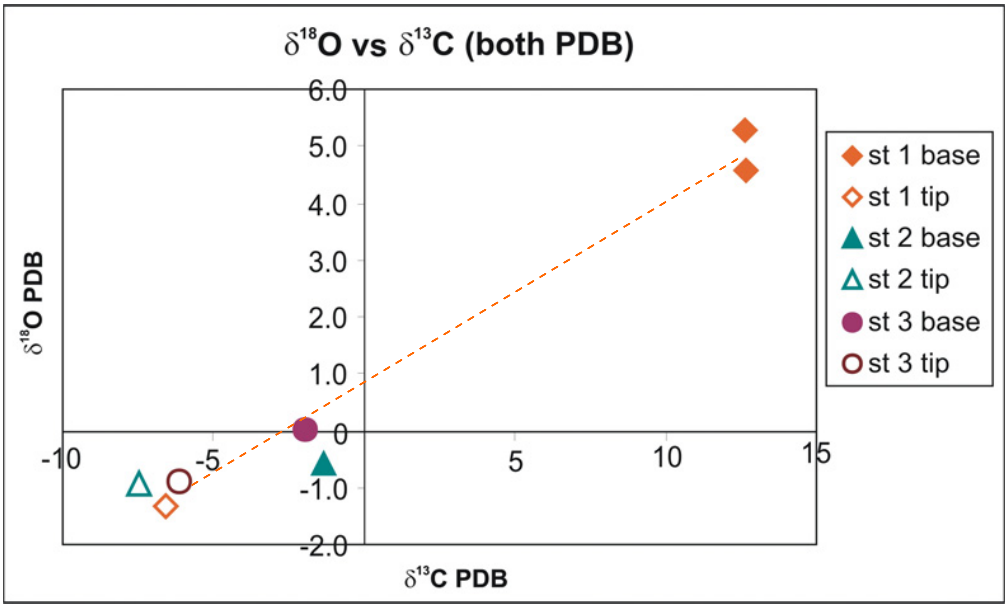

Figure 5.4. $\delta^{13}C$ and $\delta^{18}O$ values for modern stalactites graphed against each other to asses the effect of kinetic fractionation. St 1 refers to stalactite sample 1 etc, the base and tip of which were analysed.

As the $\delta^{13}C$ from Stalactite 1 is so massively enriched (Figure 5.4; Table 5.3) this stalactite was re-sampled and re-run. The $\delta^{13}C$ and $\delta^{18}O$ values of the tip of this stalactite are significantly depleted (Figure 5.4; Table, 5.3). The linear pattern of this stalactite's data (orange dashed line in Figure 5.4) suggests that kinetic fractionation was occurring during the precipitation of this stalactite, which, as the stalactite grew down towards the tip, drove both the carbon and oxygen values negative. Kinetic fractionation obscures the original signature of both carbon and oxygen and this sample was therefore discarded.

Stalactites 2 and 3 produced results similar to each other (Figure 5.4; Table 5.3). $\delta^{13}C$ values range from ~-1.4‰ at the base to between -6 and -7‰, and $\delta^{18}O$ values range from between 0 and -0.6‰ at the base to -0.9‰ at the tip. Both stalactites show marked depletion in carbon and, to a lesser extent, oxygen from the base to the tip. There is no straightforward explanation for this trend. A variety of fractionation factors, including evaporation and kinetic fractionation during precipitation, may be responsible. The spread of the data, without a clear linear trend, however suggests that kinetic fractionation did not play a major role during the precipitation of these stalactites, but rather that some unknown type of fractionation is responsible for the observed base-to-tip depletion. The results from these two stalactites confirm the already held belief that stalactites are not good reservoirs of palaeoenvironmental information, as the factors controlling the signal in modern samples cannot be easily or well constrained. These stalactite data are, therefore, not discussed any further.

5.4 Western Face 1 samples

5.4.1 Data

Samples of breccia and flowstone taken from the Western Face 1 (Figure 2.1) were analysed for carbon and oxygen isotopes and the results are summarised in Table 5.4 and shown graphically in Figure 5.6.

Sample	**Comment**	**Wt (mg)[c]**	**SA44[V][d]**	**Raw $\delta^{13}C$ vs PDB**	**Corrected[e] $\delta^{13}C$ vs. PDB[f]**	**Raw $\delta^{18}O$ vs. PDB**	**Corrected[e] $\delta^{18}O^{g}$ vs. PDB**
RP 1[r]	Fs: FBI 2 top	0.083	6.862	2.636	**-6.0**	-2.315	**-3.9**
RP 1[a]	Fs: FBI 2 top	0.072	4.295	2.724	**-5.9**	-1.890	**-3.5**
RP 2[r]	Breccia: LK	0.079	3.392	8.004	**-0.8**	-2.063	**-3.7**
RP 3[r]	Breccia: BM	0.082	3.121	7.062	**-1.7**	-1.927	**-3.5**
RP 3[r]	Breccia: BM	0.081	3.775	7.709	**-1.1**	-2.052	**-3.7**
RP 5	Fs: SR stalagmite	0.078	5.748	2.375	**-6.3**	-2.178	**-3.8**
RP 4	Fs: SR lower	0.078	5.671	0.822	**-7.8**	-2.919	**-4.5**
RP 6[r]	Breccia: SR	0.085	4.005	3.740	**-5.0**	-1.653	**-3.3**
RP 7	Fs: JS lower	0.078	5.246	3.316	**-5.4**	0.164	**-1.6**
RP 8	Breccia: JS	0.077	2.777	3.847	**-4.8**	-2.434	**-4.0**
RP 8[a]	Breccia: JS	0.077	2.843	3.849	**-4.8**	-2.428	**-4.0**
RP 8[r]	Breccia: JS	0.083	4.088	3.724	**-5.0**	-2.356	**-3.9**
RP 9	Fs: HL lower	0.078	5.867	4.804	**-3.9**	-2.750	**-4.3**
RP 10	Breccia: HL	0.078	3.214	4.602	**-4.1**	-2.336	**-3.9**
RP 11	Fs: FN lower	0.073	5.612	2.671	**-6.0**	-2.516	**-4.1**
RP 12	Breccia: FN	0.073	2.900	5.191	**-3.5**	-3.505	**-5.0**
RP 13	Fs: FN top	0.083	6.620	2.919	**-5.8**	-1.547	**-3.2**
RP 13[a]	Fs: FN top	0.084	6.818	2.885	**-5.8**	-1.576	**-3.2**
RP 13[b]	Fs: FN top	0.082	5.861	2.933	**-5.7**	-1.471	**-3.1**

a,b Addition samples run

c Initally 0.075mg of samples was weighed; this was later increased to between 0.080 and 0.085 mg for the samples with low initial voltages.

d, r Samples producing voltages of under 2 V were re-run, with an increased mass of ~ 0.080 mg per samples

e Raw data corrected from calibration curves generated from standards Cavendish Marble, Carrara Z and NBS 18

f $\delta^{13}C = (R_{sample}/R_{ref} - 1) \times 1000$, where $R = {}^{13}C/{}^{12}C$

g $\delta^{18}O = (R_{sample}/R_{ref} - 1) \times 1000$, where $R = {}^{18}O/{}^{16}O$

Table 5.4. Stable Light Isotope data for flowstone and breccia samples from the Western Face 1, sections 3 and 4, Gladysvale Cave.

Kinetic fractionation poses a serious problem in stable light isotope studies, as if kinetic fractionation occurs during the precipitation of a flowstone or the calcium carbonate cementing a breccia, the original $\delta^{13}C$ and $\delta^{18}O$ signals will be obscured and overprinted. To test for kinetic fractionation $\delta^{13}C$ and $\delta^{18}O$ are graphed against each other (Figure 5.5). If kinetic fractionation had occurred, the $\delta^{13}C$ and $\delta^{18}O$ values would be related to each other and the plot of $\delta^{13}C$ vs $\delta^{18}O$ would produce a straight line.

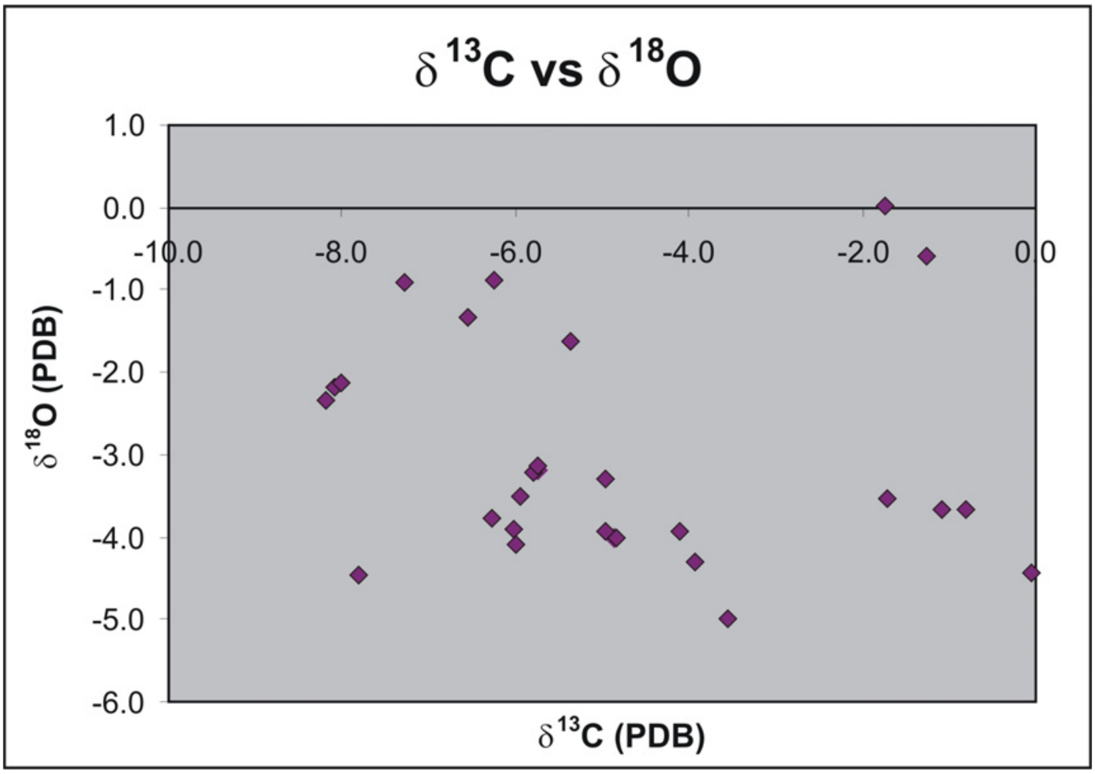

Figure 5.5. $\delta^{13}C$ against $\delta^{18}O$ for flowstone and breccia samples from the Western Face 1.

There is no clear linear trend in the data shown in Figure 5.5, indicating that kinetic fractionation has not played a role during the precipitation of the calcium carbonate in the breccias and flowstones, and that the $\delta^{13}C$ and $\delta^{18}O$ signals of these samples represent the conditions outside the cave.

Three samples, RP3, RP7 and RP13 were analysed two or three times to determine the reproducibility of the data (Table 5.4). There is a 0.1- 0.2‰ difference between re-runs of samples, such as RP7 and RP13 (with the exception of sample RP3, which shows a 0.6‰), indicating that the data is reproducible and reliable.

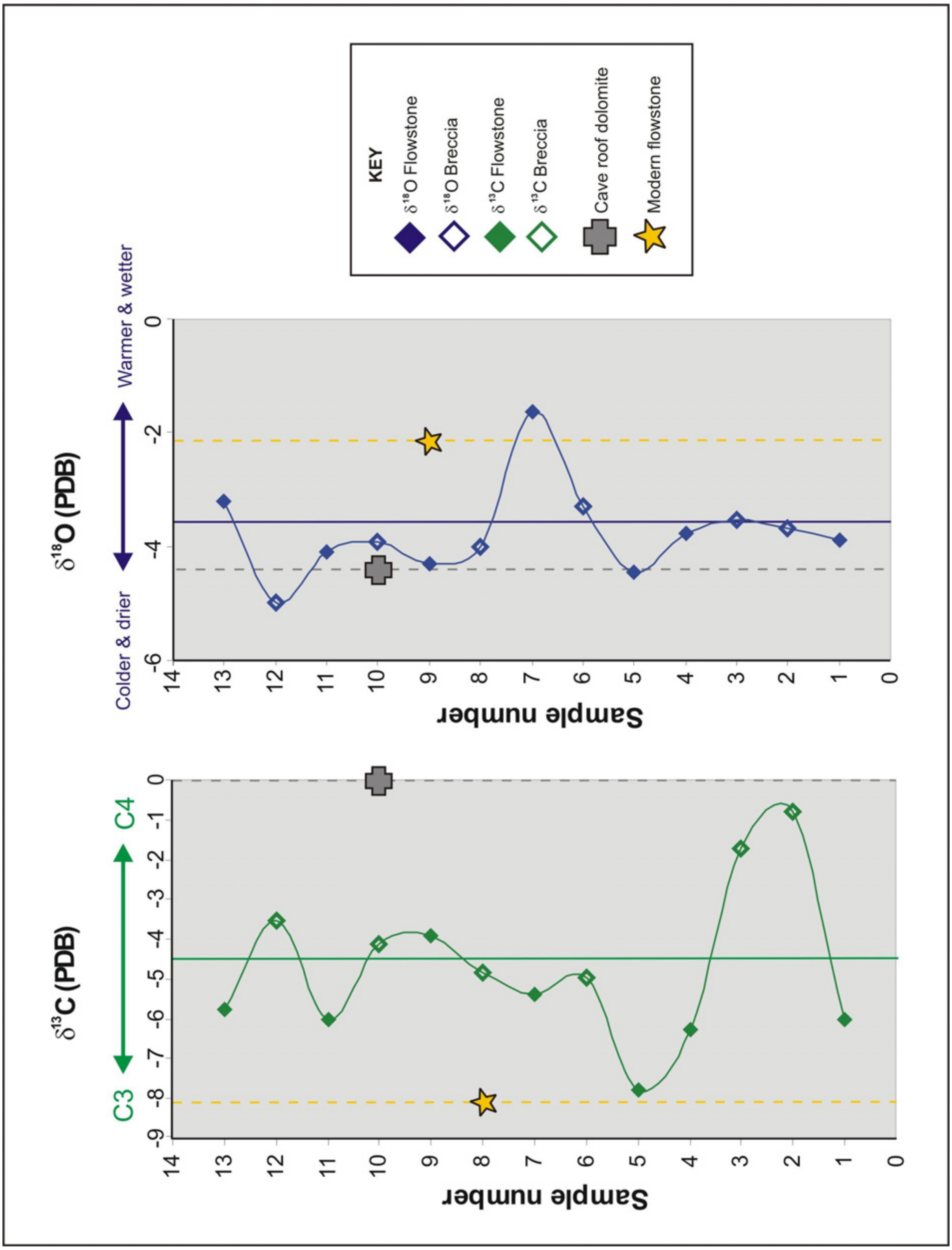

Figure 5.6. Carbon and Oxygen data of flowstone and breccias from the Western face 1, modern flowstone and cave roof dolomite, graphed against sample number. The isotopic values of the cave roof dolomite and modern flowstone are included in the graphs, but placed at a random interval, and have no relation to sample number.

5.4.2 Carbon isotopes

The $\delta^{13}C$ data for the flowstones and breccias from the Western Face 1 are summarised in Table 5.4 and Figure 5.6. In general the $\delta^{13}C$ signal shows significant variability with a saw tooth pattern (Figure 5.6). The source of the carbon signal is inherently different for the breccias and flowstones, as the breccias consist of re-mobilised soil washed directly into the cave, while the flowstones grow from drip waters, which percolate down from the soil through the cave roof dolomite. The breccias therefore sample the outside vegetation more directly and contain a less diluted signal than the flowstones. The $\delta^{13}C$ of the breccias is therefore most likely to reflect directly the vegetation growing outside the cave at the time of breccia formation. The $\delta^{13}C$ signal of the flowstones requires more interpretation owing to the more complex route followed by the drip waters and the number of different factors active during flowstone precipitation. The detailed data for the breccias and flowstones will be discussed separately.

$\delta^{13}C$ Breccia

Overall the breccias give a more enriched (more positive) signal than the flowstones, with values ranging from -0.8 to -5.8‰, with an average value of -3.4‰ (Table 5.4). As discussed above, the $\delta^{13}C$ signal of the breccias is most likely reflecting the vegetation outside the cave. Talma and Vogel (1992) estimate the abundance of C_4 plants based on the $\delta^{13}C$ signature, with +1.2‰ signifying 100% C_4 vegetation. Using this estimation, the average $\delta^{13}C$ signal of the breccias equates to 70% C_4 vegetation, indicating that C_4 grasses were the dominant vegetation type outside the cave during the periods of breccia formation. Samples RP2 and RP3, which are from the oldest breccias, LK and BM, have the least negative $\delta^{13}C$ values of between -0.8 and -1.7‰, indicating over 80% C_4 grasses. The middle breccias, SR and JS, samples RP6 and RP8, have more depleted $\delta^{13}C$ values of -4.8 and -5.0‰, indicating less C_4 grasses, at around 50% cover. The youngest breccia, HL and FN, samples RP10 and RP12, have slightly more enriched $\delta^{13}C$ values of -4.1 and -3.5‰, indicating an increase in C_4 cover to ~60%.

Therefore, the breccias at Gladysvale give a $\delta^{13}C$ signal which, using the estimation of Talma and Vogel (1992), suggest a dominant C_4 grass vegetation outside the cave duirng times of breccia formation. This C_4 signal changes through time, from ~ 80% in the older breccias, down to 50% in the middle aged breccias and back up to ~60% in the youngest breccias.

$\delta^{13}C$ Flowstone

The carbon signal from the flowstones is in general much more depleted (more negative), with $\delta^{13}C$ values ranging from -3.9 to -7.8‰ (Table 5.4). The average $\delta^{13}C$ value of the flowstones is -5.9‰, which is significantly depleted compared to the average $\delta^{13}C$ value of -3.4‰ for the breccias. Speleothems grow from cave drip waters, which source carbon from three major areas atmospheric C; decaying organic matter and root respiration in soil above the cave; and dissolved limestone (or dolomite) along the flow route to the cave (Richards & Dorale, 2003). The $\delta^{13}C$ signal in speleothems therefore reflects a mixture of factors active during calcium carbonate precipitation, including the net isotopic composition of the dissolved HCO_3^- and the precipitated $CaCO_3$, the kinetic fractionation factors in the H_2O–$CaCO_3$–CO_2 system, the saturation state of $CaCO_3$, the rate of exchange with the gaseous phase and the rate of precipitation (Richards & Dorale, 2003). Richards & Dorale (2003) explain that the interplay between these factors produces a complex system controlling the $\delta^{13}C$ signal in speleothems, and while changes in rainfall and temperature can cause variation in $\delta^{13}C$ records, the most useful information derived from speleothem $\delta^{13}C$ records relates to vegetation changes.

The Talma and Vogel (1992) vegetation estimation based on the $\delta^{13}C$ signal focuses predominantly on C_4 vegetation, but they do include C_3 estimates and argue that $\delta^{13}C$ values of -12‰ indicate 100% C_3 trees and temperate grasses. Based on this, their estimation of say 20 % C_4 from a $\delta^{13}C$ value of -8‰, equates to 80% C_3.

There is less variation between flowstone samples than that seen in the breccias. The oldest flowstone of the lower stalagmite (RP1) has a $\delta^{13}C$ value of ~-6‰, which indicates a ~60% C_3 vegetation outside the cave during flowstone formation. The flowstone and small stalagmite belonging to unit SR (RP 4 and RP 5) have slightly more depleted $\delta^{13}C$ values of between -6.3 and -7.8‰, indicating an increased C_3 cover of ~75%. The middle flowstones of units JS and HL (RP 7 and RP 9) have significantly enriched $\delta^{13}C$ values of -5.4 and -3.9‰ respectively, which indicate a drop in C_3 cover to between 55 and 40%. The uppermost flowstones binding unit FN (RP 11 and RP 12) revert back to more depleted values of between -6.0 and -5.7‰, indicating an increase in C_3 cover to ~ 60%.

$\delta^{13}C$ Discussion

The $\delta^{13}C$ values of the breccias and flowstones at Gladysvale are interpreted as representing changes in the vegetation growing outside the cave, which according to Richards and Dorale (2003), plays the most important role in determining the $\delta^{13}C$ signal of speleothems. While the source of the carbon signal is more direct in the breccias than the flowstones, the breccias still give a more enriched $\delta^{13}C$ signal, which is interpreted as representing a greater C_4 grass cover above the cave during periods of breccia formation. The flowstones give a more depleted $\delta^{13}C$ signal, which, although it is inherently a more indirect signal than the breccias, is interpreted as representing a vegetation of more C_3 trees and temperate grass growing outside the cave during conditions conducive to speleothem growth.

The modern flowstone (sample RP 20) currently growing at Gladysvale yielded $\delta^{13}C$ values of ~-8.1‰, suggesting a 30% C_3 vegetation outside the cave, using the Talma and Vogel (1992) vegetation estimates from the $\delta^{13}C$ signal. The modern vegetation of the Skeerpoort River valley has been described as ranging from "open grassland with scattered trees and bushes, to more densely wooded valleys" (Avery, 1995). Gladysvale Cave is on the sheltered eastern side of the valley, which is covered by trees and shrubs, with a grass component. The higher ground above the cave is grass-dominated. The $\delta^{13}C$ signal of the modern flowstone is therefore a fair representation of the outside vegetation.

This interpretation of the $\delta^{13}C$ signal from Gladysvale cave must be viewed with some caution, as the carbon system in caves is complex and multi-faceted. As already hinted, the passage of the ground water through the cave roof has an impact on the carbon signal of the resulting speleothems (Richards & Dorale, 2003). As $\delta^{13}C$ of the dolomitic cave roof is 0‰ (as expected for marine carbonates), it may be flattening out the signature for the flowstones growing inside the cave, as the flowstones are fed directly by the drip waters, which are sourced from the ground waters percolating through the roof. This flattening out effect would draw the carbon signal of the flowstones across to the C_3 side, and thereby underestimate the amount of C_4 in the signal. This problem is most prevalent in the flowstones, as the breccias, consisting of remobilised soil from outside the cave, contain a more direct carbon signature, which has not been filtered through the cave roof, and is a more direct reflection of the vegetation outside the cave. However, the saw-tooth nature of the data does suggest that there are real differences in the carbon signal between the breccias and flowstones, and that these excursions may be underestimated for the flowstones, and the C_3 cover estimates should be viewed as minimum estimates.

Having established that the carbon signal is reflecting changes in vegetation, the different types of vegetation growing above the cave can serve as palaeoclimatic proxies. Vogel (1993) relates the modern geographical distribution of C_3 and C_4 plants in southern Africa to different climatic zones. In general, winter rainfall regions are dominated by C_3 plants (trees and shrubs), while warm, arid summer rainfall areas, such as that around the Cradle of Humankind World Heritage Site, are 95–100% C_4. The presence of C_4 grass in the past cannot be simply interpreted as signifying more arid conditions, but rather that the overall conditions at that time favoured C_4 over C_3 vegetation. Vogel (1993) argues that C_4 grasses are adapted to more seasonal rain and high radiation causing higher temperatures during the growing season and grow preferentially where the growing season temperatures are above 22°C and not below 8°C (Vogel *et al.,* 1978; Ehleringer *et al*., 1997). C_4 plants have also been shown to out-compete C_3 grasses when atmospheric CO_2 levels are low (Cerling *et al*., 1997). C_3 plants (trees and temperate grasses) need increased rainfall - preferably less seasonal to grow (Vogel *et al.,* 1978; Ehleringer *et al*., 1997), and a C_3 signal can therefore be used to infer these conditions in the past. Thus the $\delta^{13}C$ signal reflects more than just the dominant vegetation type, but changes in atmospheric CO_2 levels, temperature, moisture conditions and seasonality of rainfall (Holmgren *et al*, 2003). Flowstones need increased effective precipitation to grow (Ayliffe *et al*., 1998), as do C_3 plants (Vogel, 1993), so it is not surprising that the Gladysvale flowstones have a $\delta^{13}C$ signal that indicates a 50 to 60% C_3 vegetation outside the cave during speleothem formation inside the cave.

5.4.3 Oxygen isotopes

The oxygen isotope data for the breccia and flowstone samples taken from the Western Face 1 are summarised in Table 5.4 and Figure 5.6. The $\delta^{18}O$ signal is, in general, much flatter than the $\delta^{13}C$ signal (Figure 5.6), with less obvious difference in $\delta^{18}O$ values between the breccias and flowstones. The $\delta^{18}O$ signal is different from the $\delta^{13}C$ signal, in that the $\delta^{18}O$ for both the breccias and flowstones is sourced from the cave drip waters as the $\delta^{18}O$

signal for the breccias comes more from the calcium carbonate cement than from the actual breccia sediments themselves.

The distribution of $\delta^{18}O$ between calcite and water during the precipitation of speleothems is temperature dependent, but only if the system remains in isotopic equilibrium, such as at the back of deep caves, where ventilation is minimal and humidity high (Richards & Dorale, 2003). Deviations in $\delta^{18}O$ in ancient calcite cannot however be attributed to temperature shifts alone, and are a function of: changes in the $\delta^{18}O$ of the sea water, which fluctuates with changing ice volumes; changes in the path of the water from the source to the site of precipitation; and the isotopic composition and amount of rain and percolating vadose waters (Richards & Dorale, 2003). In some cases calcite deposited during interglacial periods has a less negative $\delta^{18}O$ signature (Gascoyne *et al.*, 1981; Goede *et al.*, 1986; Dorale *et al.*, 1992; Lauritzen, 1995). In general, negative shifts in $\delta^{18}O$ values are attributed to a combination of factors, including glacial-interglacial changes in ocean $\delta^{18}O$, intensification of rainfall and seasonal patterns of rainfall, which may result in shifts too great to be attributed to temperature alone (Richards & Dorale, 2003). So, as with carbon, the $\delta^{18}O$ signature of speleothems is a product of a complex system, with no simple interpretation.

$\delta^{18}O$ Breccia

The $\delta^{18}O$ data for the breccias (Table 5.4; Figure 5.6) shows very little variation, with a range of only -1.7‰ from -3.3 to -5.0‰. The average values for the breccias is -3.9‰, which is only slightly depleted compared to the average value of -3.5 for the flowstones. These data are difficult to interpret, as there are few published studies of the $\delta^{18}O$ values for cave breccias. The $\delta^{18}O$ signal in flowstones is better understood and quantified.

$\delta^{18}O$ Flowstone

The $\delta^{18}O$ signal in Gladysvale flowstones (Table 5.4; Figure 5.6) show a greater range than the breccias, with values from -1.6 to -4.5‰. The average $\delta^{18}O$ value for the flowstones is -3.5. However, sample RP 7 is very positive at -1.6‰, and stands out from the other data. The modern flowstone at Gladysvale Cave is growing under very evaporative conditions from the increased air circulation in the cave, due to the enlarging of the entrances by the lime miners, and produced an enriched $\delta^{18}O$ signal of ~-2.4‰. Flowstone RP 7 could not be dated via U-series because of the high degree of detrital contamination. According to Moriarty *et al*. (2000) this signifies an open cave, which would increase the possibility of evaporation inside the cave. Thus, the highly enriched $\delta^{18}O$ value of RP 7 is most likely a product of evaporation, and is consequently exaggerated. Without RP7, the average value is -3.8‰, and this is taken to be more representative of the $\delta^{18}O$ signal for the flowstones. Using this -3.8‰ average value, the flowstones are on average slightly more enriched than the breccia samples. This enrichment is not easy to interpret in isolation, because of the many factors determining the $\delta^{18}O$ signal of speleothems,

Holmgren *et al*. (2003) interpret the $\delta^{18}O$ of the T8 stalagmite from Makapansgat, 200 km to the north-east of Gladysvale and the Cradle of Humankind World Heritage Site, as reflecting changing types of precipitation. The $\delta^{18}O$ in precipitation is controlled by the Rayleigh distillation of atmospheric vapour, which is driven, primarily, by changes in the air-mass temperature (Rozanski *et al*., 1993). Therefore changes in $\delta^{18}O$ are a consequence of changes in the frequency of different types of precipitation, namely persistent mid altitude rain and intense convective, high altitude storm events (Holmgren *et al*., 2003). High altitude, convective storms have depleted $\delta^{18}O$ values (Rozanski *et al*., 1993) and increase in frequency during relatively dry summers (Harrison, 1986). In southern Africa, drier and more arid conditions in the northern summer rainfall areas are associated with the equatorward expansion of the atmospheric circumpolar vortex (Tyson, 1986; Tyson & Preston-Whyte, 2000). The poleward expansion of the tropical circulation that accompanies a contraction of the atmospheric circumpolar vortex has the opposite effect, and is associated with warmer, wetter conditions (Tyson, 1986; Tyson & Preston-Whyte, 2000). Thus, Holmgren *et al*. (2003) interpret the depleted, lower $\delta^{18}O$ values as reflecting drier periods, with reduced average annual rainfall, compared to wetter years, during which thunderstorms and hail increase in frequency, as does the amount of rain in a single rainfall event. Therefore, the type of rain (storms and hail) and the amount of rain (large amounts in a single event, but less on an average annual basis) produce the depleted $\delta^{18}O$ values in the T8 stalagmite. Conversely, the less depleted (more positive) $\delta^{18}O$ values are related to wetter conditions, with a high frequency of persistent, warm rain from middle-level stratiform cloud bands (Holmgren *et al*., 2003).

Within the framework developed by Holmgren *et al*. (2003), the slightly less negative $\delta^{18}O$ values of the Gladysvale flowstones can be interpreted as signalling warmer, wetter conditions, during which rainfall was less seasonal and more persistent. However, there is no consistent relationship between the $\delta^{18}O$ values of the flowstone and breccias, as towards the base of the sequence, samples RP2 to RP6 produce a range of $\delta^{18}O$ values, with slightly *more* depleted values for the flowstones, not the breccias (Table 5.4)

$\delta^{18}O$ Discussion

According to Holmgren *et al*. (2003) warmer and wetter periods produce more enriched $\delta^{18}O$ values, while cooler drier periods produce more depleted $\delta^{18}O$ values. This interpretation can be applied successfully to the Gladysvale samples, as the flowstones do show slightly more enriched $\delta^{18}O$ values than the breccias. However, the differences between the $\delta^{18}O$ values of the breccias and flowstones are so minute (an average of 0.1‰) that other factors controlling the $\delta^{18}O$ values of the Gladysvale samples must be examined.

The $\delta^{18}O$ value of -4.4‰ for the dolomite cave roof plots in the middle of the narrow spread of the $\delta^{18}O$ values of the flowstones and breccias from inside the cave (Figure 5.6). This close relationship suggests that the dolomite oxygen signal may be flattening out the signal from the breccias and flowstones. The flattening out of the oxygen signal may, therefore, be caused by the passage of groundwater through the cave roof, where it inherits the dolomite signature. Vogel and Talma (1992) have a similarly flat oxygen curve derived from the Cango Cave stalagmite. They attribute the flatness of the oxygen signal to the residence time of the ground waters above the cave, during which the original signal of the rain is lost or obscured.

The average $\delta^{18}O$ signal of the rainfall measured in Pretoria (~45km from Gladysvale) from 1958-1985 is -3.7‰ (IAEA, 1992), which is the same as the average value of the ancient Gladysvale flowstones (Table 5.4). The modern flowstone at Gladysvale has a $\delta^{18}O$ value of ~-2.2‰, but as already discussed, this value is most likely a product of the evaporative conditions inside the cave, rather than a reflection of the current climate. Holmgren *et al*. (2003) report drip water $\delta^{18}O$ values of -4 ‰, and groundwater $\delta^{18}O$ values from -3.6 to -5.2 ‰ from the nearby Bela-Bela (formally Warmbaths) hot springs. These values for the modern rain in Pretoria, the groundwater at Bela-Bela, the cave roof dolomite at Gladysvale and the cave drip waters at Makapansgat all fall within the same relatively narrow range, of ~-3.7 to ~4.5‰. The $\delta^{18}O$ signal of the flowstones at Gladysvale are a product of all these variables, the rain, groundwater, the cave roof rock and the cave drip waters, and the $\delta^{18}O$ values of these will have an influence of the resulting speleothems. The lack of any clear patterning between the $\delta^{18}O$ values of the Gladysvale flowstones and breccias (unlike the $\delta^{13}C$ values, which do show clear partitioning) suggests that the contributing sources of $\delta^{18}O$ signal have defined the $\delta^{18}O$ values of the Gladysvale speleothems, and as a result flattened out the signal and removed the climatically controlled component seen in the T8 stalagmite. Thus, the $\delta^{18}O$ signal of the flowstones and breccias at Gladysvale Cave is *not* a useful palaeoclimatic proxy on its own.